

Spatial and temporal variability of methane emissions and environmental conditions in a hyper-eutrophic fishpond

Petr Znachor^{1,2}, Jiří Nedoma¹, Vojtech Kolar^{1,2}, Anna Matoušů¹

¹Biology Centre of Czech Academy of Sciences, v.v.i., Institute of Hydrobiology, Na Sádkách 7, České Budějovice, 37005, Czech Republic

²Faculty of Science, University of South Bohemia, Branišovská 1760, České Budějovice, 37005, Czech Republic

Correspondence to: Anna Matoušů (anna.matousu@gmail.com)

Abstract. Estimations of methane (CH₄) emissions are often based on point measurements using either flux chambers or a transfer coefficient method which may lead to strong underestimation of the total CH₄ fluxes. In order to demonstrate more precise measurements of the CH₄ fluxes from an aquaculture pond, using higher resolution sampling approach we examined the spatiotemporal variability of CH₄ concentration in the water, related fluxes (diffusive and ebullitive) and relevant environmental conditions (temperature, oxygen, chlorophyll-a) during three diurnal campaigns in a hyper-eutrophic fishpond. Our data show remarkable variance spanning several orders of magnitude while diffusive fluxes accounted for only a minor fraction of total CH₄ fluxes (4.1–18.5 %). Linear mixed-effects models identified water depth as the only significant predictor of CH₄ fluxes. Our findings necessitate complex sampling strategies involving temporal and spatial variability for reliable estimates of the role of fishponds in a global methane budget.

Keywords: aquaculture, emissions, fishpond, freshwater, heterogeneity, methane

23 **1 Introduction**

24 Freshwater aquaculture ponds (fishponds) represent man-made counterparts to natural shallow lakes (Scheffer,
25 2004) which are mainly used for fish production (mostly of common carp, *Cyprinus carpio* L.) and water retention
26 in the landscape. Fishponds serve also as secondary biotope for various organisms (Kolar et al., 2021), supporting
27 noteworthy animal and plant diversity (Pokorný and Hauser, 2002). However, most fishponds suffer from high
28 fish stock densities, excessive carbon and nutrient loading from supplemental fish feeding, sewage pollution, and
29 fertiliser runoffs from agricultural catchments or nutrient mobilisation from the anoxic sediment layers (Pechar,
30 2000). As a result, the trophic structure of plankton communities has shifted towards a reduction of large
31 zooplankton and massive development of phytoplankton, especially cyanobacterial blooms (Potužák et al., 2007),
32 limiting light penetration in the water column. Rapid changes in the intensity of biological processes such as
33 photosynthesis and respiration often result in pronounced daily or seasonal fluctuations in dissolved oxygen (Baxa
34 et al., 2021), signalling decreasing ecosystem stability. The extent of anoxia, accumulation of organic biomass,
35 and rapid heating of the shallow water during summer result in enhanced production of greenhouse gases (Grasset
36 et al., 2018, Zhang et al., 2021; Bartosiewicz et al., 2021).

37 Most concerning are CH₄ emissions as freshwater aquaculture systems release more than 6 Tg CH₄ yr⁻¹ (Yuan et
38 al., 2019). Methane can be emitted via several pathways: simple molecular diffusion, ebullition (in the form of
39 bubbles released from oversaturated sediments), plant-mediated flux (Bastviken et al., 2004), but also through so
40 far neglected pathways including aeration, emissions from dry/drying sediments, or dredged organic material
41 (Kosten et al., 2020). Among all, ebullition is considered the dominant pathway (van Bergen et al., 2019; Kosten
42 et al., 2020), which can contribute 50–96 % (Casper et al., 2000; Xiao et al., 2017; van Bergen et al., 2019; Yang
43 et al., 2020; Zhao et al., 2021) to the total CH₄ flux. Along with the second important pathway – molecular
44 diffusion, both exhibit high spatiotemporal variability due to various physical and biological factors acting on very
45 short time scales, for instance, temperature (van Bergen et al., 2019), nutrient loading (Zhang et al., 2021), CH₄
46 production rates (Zhou et al., 2019), CH₄ oxidation rates (Sanseverino et al., 2012), dissolved oxygen concentration
47 (Xiao et al., 2017), management regime (Yang et al., 2019), or the quality of organic matter in the sediment
48 (Schmiedeskamp et al., 2021). Recently, the potential involvement of phytoplankton in CH₄ production and
49 emissions has been suggested (Yan et al., 2019; Bižić et al., 2020; Bartosiewicz et al., 2021). The complex
50 interactions between physical and biological factors lead to a dynamic and ever-changing environment,
51 characterised by high spatial and temporal variability of methane fluxes in ponds.

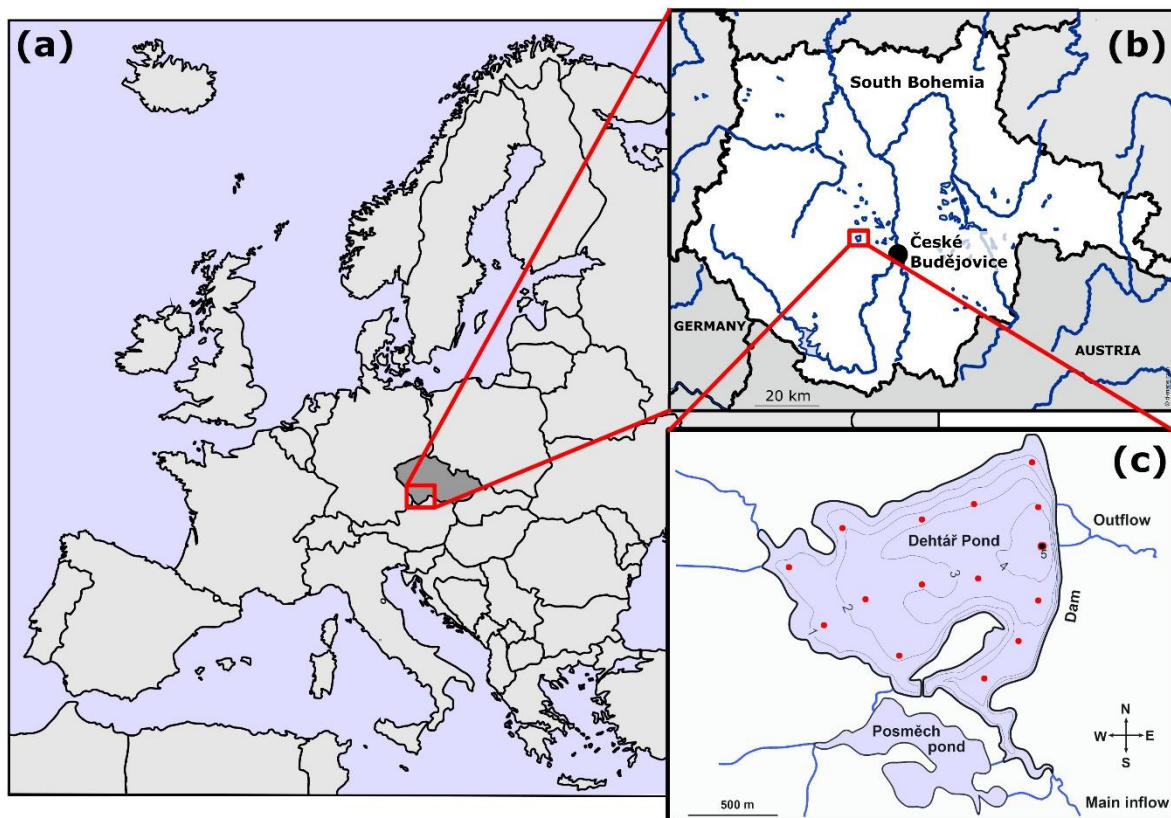
52 Although fishponds are recognised as powerful model systems for studies in ecology and evolutionary or
53 conservation biology (De Meester et al., 2005; Céréghino et al., 2008), the extent of environmental heterogeneity
54 in fishponds and shallow inland small waterbodies remains poorly understood (Ortiz and Wilkinson, 2021), largely
55 because the driving factors are either system-specific or highly variable on short time scales (Laas et al., 2012).
56 Most of current information on lentic ecosystem structure and function comes from single-site sampling, in which
57 measurements are taken over time at the deepest point in the lake, which does not sufficiently account for within-
58 lake spatial variation (Stanley et al., 2019). The motivation for our study was the growing concern about the role
59 of fishponds as important sources of CH₄ fluxes to the atmosphere (Wik et al., 2016). Unfortunately, the majority
60 of global CH₄ flux estimates rely on upscaling methods (DelSontro et al., 2018a) based on a limited number of
61 measurements that do not account for diurnal and seasonal variability or ecosystem spatial heterogeneity. Yang et
62 al. (2019) indicates that a larger number of spatial replicates over a number of months is mandatory to improve
63 the accuracy of whole-pond CH₄ flux estimates. The published research from other aquaculture studies have been
64 performed mainly in tropical and subtropical zones in fish or crab aquacultures (e.g. Hu et al., 2016; Ma et al.,
65 2018; Yang et al., 2019, 2020; Yuan et al., 2019, 2021). To better understand the spatial dynamics of CH₄ fluxes
66 and environmental heterogeneity in temperate freshwater shallow lake, we conducted a spatial sampling of the
67 hyper-eutrophic Dehtář fishpond (Czech Republic, Europe). Since the seasonal CH₄ production is strongly affected
68 by temperature, we focused on warm summer months where the total CH₄ fluxes were expected to be the highest
69 (Jansen et al., 2019). The objectives of our study were (i) to determine the spatial heterogeneity of CH₄ diffusive
70 and total fluxes and fundamental limnological variables (oxygen, temperature, chlorophyll-a) and their change
71 daily and monthly in the hyper-eutrophic pond, and (ii) to identify the factors that influence CH₄ fluxes to improve
72 our understanding of the importance of spatiotemporal variability for global estimates of CH₄ efflux to the
73 atmosphere.

74 **2 Material and Methods**

75 **2.1 Study site description**

76 The Dehtář fishpond (49°00'24.4"N 14°17'39.3"E) is a shallow man-made lake (average and maximum depth: 2.4
77 and 6 m) constructed in 1479 (Potužák et al., 2016). It is used for polycultural, semi-intensive production of
78 common carp, which account for 90–95 % of the fish biomass (Rutegwa et al., 2019). The pond is stocked with
79 two-year old carp harvested at the end of a two-year production cycle. To increase fish production, the original

80 management, based mainly on natural processes, has been intensified, and today manuring and supplementary
81 feeding in the form of grain or fish pellets, are common practices (Pechar, 2000). The pond lies in a flat agricultural
82 landscape at 406.4 m above sea level in the upper Vltava River basin in South Bohemia (Czech Republic) which
83 is characteristic with its network of fishponds (Fig. 1b). Due to the orography of the landscape, the Dehtář fishpond,
84 surrounded by narrow belts of littoral vegetation and adjacent to grassland and arable land, is exposed to wind,
85 mainly from the northwest (for aerial photograph, see Suppl. Fig 1). The catchment area is 91.4 km². The main
86 inflow is the Dehtářský stream in the south, while several smaller tributaries flow in from the west (Fig. 1c). The
87 fishpond has a dam 234 m long and 10 m high, with two outlets and a safety spillway. Covering 2.28 km², the
88 Dehtář fishpond is among the ten largest fishponds in the Czech Republic, holding a volume of 4.71×10^3 m³ and
89 having a water residence time of 146–445 days (Potužák et al., 2016).



90

91 **Figure 1.** Location (a, b; copyright www.d-maps.com; https://d-maps.com/carte.php?num_car=2232&lang=en and https://d-maps.com/carte.php?num_car=265046&lang=en; modified) and bathymetric map (c; credit Jiří Jarošík) of the sampled Dehtář
92 fishpond: blue lines indicate hydrological connections; red dots representing the sampling points. Highlighted sampling point
93 at the dam depicts the deepest site where vertical profiles were measured. Numbers indicate isobath depth.
94

95

96 2.2 Sampling design and measurement

97 To measure spatial heterogeneity and temporal changes in limnological parameters and methane fluxes, we
98 conducted three 36-hour surveys in summer 2019 (July 2–3, August 13–14, September 19–20). In the morning

99 (between 5–6 a.m.), we first measured surface values and vertical profiles of temperature, oxygen, and chlorophyll-
100 *a* concentration at the deepest point (see below for details). We subsequently installed 15 floating polyethylene
101 chambers (as shown in Fig. 1c), serving as fixed sampling sites and at the same time for accumulation of CH₄
102 fluxes (see further), starting in the western part of the fishpond. During installation (and further during each
103 sampling), temperature, pH, and oxygen concentration were measured at 0.3 m depth using the WTW 330i pH
104 meter and Oximeter (WTW, Weilheim, Germany). Vertical chlorophyll-*a* profiles were measured at each sampling
105 site using a submersible fluorescence probe (FluoroProbe, bbe Moldaenke, Kiel, Germany). From each site, the
106 average chlorophyll-*a* concentration in the surface layer (0–1 m depth) was used to assess the phytoplankton spatial
107 heterogeneity.

108 To minimise the chance that the differences observed among sites were due to time of day, we conducted repeated
109 measurements at the deepest point at the end of each sampling. This was relevant mainly to the initial measurement,
110 when the installation of all floating chambers took a total of 3 hours and 50 minutes. All other measurements, i.e.,
111 the interval between the first and last sampling point, required approximately two hours each. If there was a change,
112 all values were corrected for the sampling time by linear interpolation:

$$113 \quad P_{corr} = P_t + (P_{end} - P_0) \times \frac{(t-t_0)}{(t_{end}-t_0)} \quad (1)$$

114 where P_{corr} is the corrected value of a parameter, P_t is its value measured at the time t , P_0 and P_{end} are parameter
115 values measured at the deepest point at the start (time t_0) and at the end (t_{end}) of the sampling. In the evening and
116 morning of the second day (roughly at 12 h intervals), we performed additional measurements of spatial
117 heterogeneity, allowing us to assess diurnal and nocturnal changes. In addition, samples for measuring CH₄
118 concentration in the surface water were collected at each site and analysed as described below. To assess diurnal
119 variations in thermal structure and oxygen concentration in the water column, we made vertical profile
120 measurements at the deepest point (Fig. 1c) at 3–6 h intervals using the YSI EXO 2 multiparametric probe (YSI
121 Inc., Yellow Springs, USA).

122 **2.3 Methane measurements**

123 Water samples for determining CH₄ concentration in the surface water were collected at all 15 sampling sites in
124 triplicates into 20 ml glass bottles. The bottles were capped bubble-free under water with black butyl rubber
125 stoppers (Ochs, Germany) and sealed with aluminium crimps. Immediately after sampling, the water samples were
126 preserved by injecting 100 μ L of concentrated sulfuric acid to stop the microbial activity (Bussmann et al., 2015).
127 The samples were processed within one week in the laboratory using a headspace technique according to
128 McAuliffe (1971). Methane concentration in the headspace was measured using an HP 5890 Series II gas

129 chromatograph (Agilent Technologies, USA) and calculated with the solubility coefficient given by Yamamoto et
130 al. (1976).

131 Methane diffusive fluxes (F) were then calculated for each sampling site indirectly using the 2-layer model with
132 the equation:

$$133 \quad F = k(C_{sur} - C_{eq}) \quad (2)$$

134 where C_{sur} is the CH_4 concentration in surface water in $\mu\text{mol L}^{-1}$, C_{eq} is the CH_4 concentration in surface water in
135 equilibrium with the atmosphere in $\mu\text{mol L}^{-1}$, and k is the CH_4 exchange constant (cm h^{-1}). The atmospheric partial
136 pressure of CH_4 was set to 1.8 ppm. To compute k values, we first derived k_{600} estimates using a wind speed-based
137 relationship according to Crusius and Wanninkhof (2003):

$$138 \quad k_{600} = 1.68 + (0.228 \times U_{10}^{2.3}) \quad (3)$$

139 where U_{10} represents the wind speed at 10 m height (in m s^{-1} ; obtained from the nearby gauging station)
140 approximated by $U_{10} = 1.22U$, where U is the wind speed at 1.5 m height. We then converted k_{600} to k using the
141 eq. 4 according to Crusius and Wanninkhof (2003):

$$142 \quad k = k_{600} \left(\frac{Sc}{600} \right)^n \quad (4)$$

143 where k_{600} is the gas transfer velocity for a Schmidt number (Sc) of 600; n is a wind speed-dependent conversion
144 factor, for which we used $-2/3$ for $U_{10} < 3.7 \text{ m s}^{-1}$ (Jähne et al., 1987). The Schmidt number for CH_4 was calculated
145 according to Wanninkhof (2014):

$$146 \quad Sc = 1909.4 - 120.78t + 4.1555t^2 - 0.080578t^3 + 0.000658t^4 \quad (5)$$

147 where t ($^{\circ}\text{C}$) is the water temperature at the time of CH_4 extraction. The parameter C_{eq} in Eq. (1) was determined
148 from the equation:

$$149 \quad C_{eq} = \beta \times pCH_4 \quad (6)$$

150 where β is the solubility coefficient of CH_4 as a function of temperature according to Wiesenburg and Guinasso
151 (1979), and pCH_4 is the partial pressure of CH_4 in the atmosphere.

152 To estimate total CH_4 fluxes from the water column to the atmosphere (i.e., diffusive and ebullitive fluxes), we
153 measured CH_4 accumulation in open-bottom floating polyethylene chambers (volume 3.1 L; area 0.024 m^2). Each
154 gas chamber was anchored at individual 15 fixed sampling sites, but allowed to float freely on the water surface.
155 Gas was accumulating for approximately 12 h (each incubation had a start and end point) during particular
156 sampling period, i.e., during the day and night periods. Afterwards, 30 ml of gas was carefully taken from each
157 chamber, after mixing the headspace in the chamber, and stored in evacuated Exetainers[®] (Labco Limited, UK).
158 Chambers were ventilated after each sampling period to reset the incubation conditions. Methane fluxes were

159 calculated as the difference between initial background and final concentration in the chamber headspace and
160 expressed on the 1 m² area of the surface level per day according to Bastviken et al. (2004).

161 **2.4 Background limnological parameters**

162 During each campaign, water samples for analysis of nutrient concentration and phytoplankton composition were
163 collected from the surface at the deepest point using a Friedinger sampler. Water transparency was measured using
164 a Secchi disk. Total phosphorus (TP) and soluble reactive phosphorus (SRP) were analysed spectrophotometrically
165 according to Kopáček and Hejzlar (1993) and Murphy and Riley (1962), respectively. Concentrations of NH₄⁺ and
166 NO₃⁻ were determined according to the procedure of Kopáček and Procházková (1993) and Procházková (1959),
167 respectively. Phytoplankton samples were preserved with Lugol's solution and examined for species composition
168 with an inverted microscope (Olympus IMT-2). Weather data were obtained from the gauging station at the
169 fishpond dam.

170 **2.5 Statistical analyses**

171 Two-tailed paired Student's t-tests and Two-way ANOVA with post-hoc Tukey's multiple comparison test (Prism
172 9.3, GraphPad Software Inc., La Jolla, USA) tested for differences between diffusive and total CH₄ fluxes between
173 day and night and among three sampling campaigns, respectively. The percentage of data variability explained by
174 different factors (daytime, month and site) was calculated with the Two-way RM ANOVA. Contour graphs
175 illustrating changes in spatial heterogeneity of measured parameters were constructed in Surfer 10 (Golden
176 Software, Inc., Colorado, USA) using the kriging contouring method. Spatial heterogeneity was quantified for
177 each sampling by calculating the spatial variance (i.e. coefficient of variation of values measured at 15 sampling
178 sites; see, e.g. Fig 2):

$$179 \quad CV\% = 100 \times \frac{SD}{mean} \quad (7)$$

180 Higher spatial variance indicates increasing ecosystem patchiness. Linear mixed-effects models were used to
181 analyse the effects of O₂, pH, temperature, and water depth on the CH₄ diffusive fluxes with the random effect of
182 time of day nested within the effect of sampling date. The most parsimonious model was obtained by a manual
183 backward selection, where we sequentially removed all insignificant predictors ($p > 0.05$) using likelihood ratio
184 tests implemented in the drop1 function (Zuur et al., 2009). We also compared the slopes of the month-specific
185 regression lines produced by the model using analysis of covariance (Zar, 1984). Linear mixed-effects models
186 were implemented in the lme4 package version 1.1-21 (Bates et al., 2015), and Kenward-Roger F-tests were

187 computed using the ANOVA Type II function from the pbkrtest package version 0.4-7 (Halekoh and Hojsgaard,
 188 2014). The prediction of the resulting final model was visualised in the package ggeffects version 0.14.1 (Lüdtke,
 189 2018). Package performance version 0.4.4 (Lüdtke et al., 2020) was used to calculate Nakagawa's R^2 of the linear
 190 model. The statistical analyses were performed using R software (v. 3.5.2, R Core Team, 2018).

191 3 Results

192 3.1 Weather and background fishpond characteristics

193 Weather parameters varied among sampling campaigns. In July, clear skies prevailed with the daily air temperature
 194 above 30 °C (Table 1). During the August and September measurements, it was very cloudy, and daily air
 195 temperatures decreased to 22 and 18 °C, respectively. The water level was stable during the whole studied period
 196 with a monthly fluctuation of ~ 10 cm. Water transparency was low (15–40 cm), with an increasing trend towards
 197 the end of summer (Table 1). Concentrations of total phosphorus and soluble reactive phosphorus were high (Table
 198 1), consistent with a hyper-eutrophic state of the fishpond. In contrast, nitrogen concentrations were rather low,
 199 with ammonium nitrogen being the predominant form of inorganic N in the water (Table 1).

200 **Table 1:** Basic characteristics of the Dehtār fishpond during the studied period, measured at the surface at the deepest point.

	July	August	September
Weather	Clear sky, windy	Partly cloudy, no wind	Partly cloudy, no wind
Air temperature (°C)	25–32	20–22	11–18
Water temperature (°C)	24–29	22–23	16–17
Maximum wind speed (m s⁻¹)	3.2	0.8	0.9
PHAR (mol m⁻² day⁻¹)	9.5	3.4	5.0
Secchi depth (cm)	15	30	40
TP (µg L⁻¹)	568	527	406
SRP (µg L⁻¹)	100	200	107
N-NH₄⁺ (µg L⁻¹)	23	783	560
N-NO₃⁻ (µg L⁻¹)	14	23	46
Chl-<i>a</i> (µg L⁻¹)	456	156	185
Phytoplankton composition	Cyanobacteria	Cyanobacteria, green algae, cryptophytes	Cryptophytes, green algae

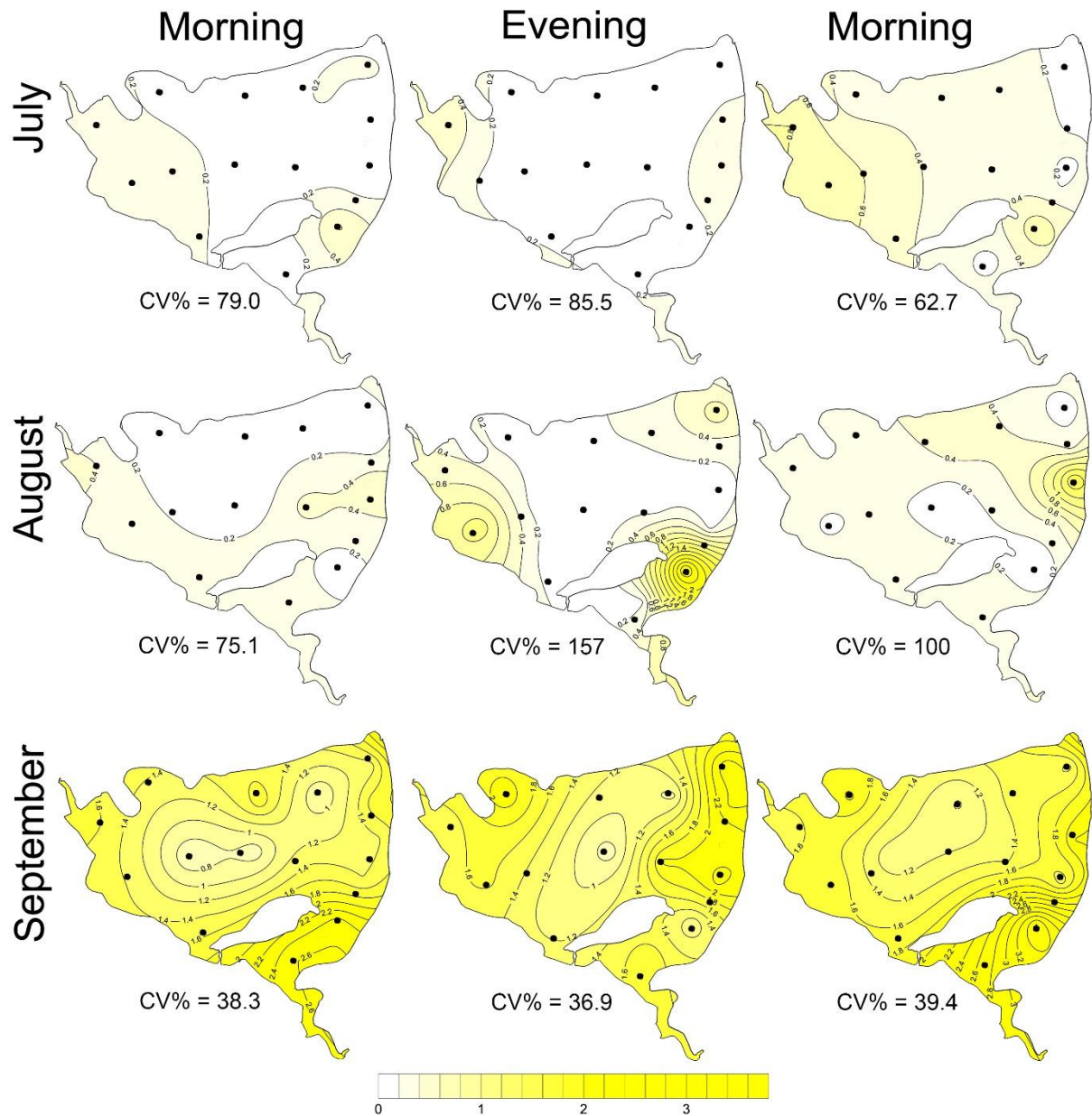
201

202 Chlorophyll-*a* concentrations were highest in July due to the dense cyanobacterial bloom accumulated at the
203 surface (Table 1). The phytoplankton consisted of only three cyanobacterial taxa: *Dolichospermum flos-aquae*,
204 *Planktothrix agardhii*, and *Raphidiopsis mediteranea*. In August, phytoplankton was more diverse but also
205 dominated by cyanobacteria: *P. agardhii*, *Aphanizomenon issatschenkoi*, and *D. flos-aquae*. In September,
206 cyanobacteria were absent and instead, cryptophytes (*Cryptomonas reflexa*), green algae (*Pediastrum*, *Coelastrum*
207 and *Desmodesmus*) and dinoflagellates (*Ceratium hirundinella*) prevailed.

208 **3.2 Methane concentration and fluxes**

209 The CH₄ concentration in surface water was highly supersaturated over the whole studied period. The obtained
210 values varied from 0.003 up to 3.75 μmol L⁻¹ (Fig. 2), which corresponded to saturation levels of 108–12 834%.
211 It is obvious, that the obtained data show remarkable variance: the mean (± SD) values were 0.22 ± 0.18 for July,
212 0.34 ± 0.45 for August, and 1.61 ± 0.61 μmol L⁻¹ for September (Suppl. Fig. 11).

213



214

215 **Figure 2:** Surface methane concentrations ($\mu\text{mol L}^{-1}$). Contour graphs illustrating both seasonal and daily changes in spatial
 216 heterogeneity (indicated by the coefficient of variation, CV%) in the fishpond. Black dots representing the sampling sites.

217

218 Diffusive fluxes (i.e., calculated from CH_4 concentration, see Eq. 2) showed the lowest values in July and August

219 (average 0.12 and $0.16 \text{ mmol m}^{-2} \text{ d}^{-1}$, respectively) and pronouncedly peaked in September (average 0.78 mmol

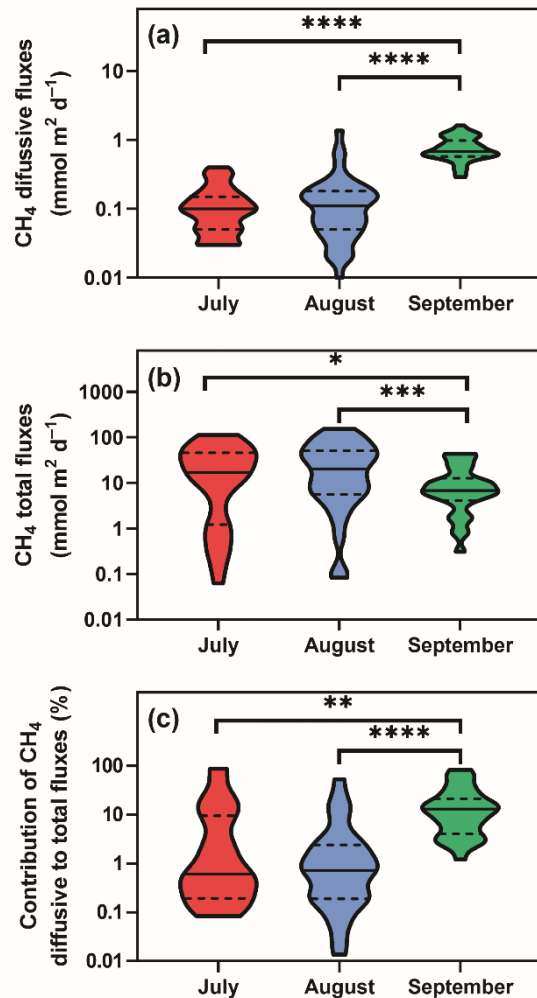
220 $\text{m}^{-2} \text{ d}^{-1}$, Fig. 3a). By contrast, in July and August, the average total CH_4 fluxes (obtained with floating chambers)

221 showed the highest values (average $31.8 \text{ mmol m}^{-2} \text{ d}^{-1}$; ranging from 0.08 to $152 \text{ mmol m}^{-2} \text{ d}^{-1}$) while in

222 September, total CH_4 fluxes were three times lower than before (average $11.8 \text{ mmol m}^{-2} \text{ d}^{-1}$, range 0.3 to 43.5

223 $\text{mmol m}^{-2} \text{ d}^{-1}$, Fig 3b). As a result, diffusive fluxes accounted for only a minor fraction of total CH_4 fluxes to the

224 atmosphere (on average, 9.2% in July, 4.1% in August, 18.5% in September, Fig. 3c).



225

226 **Figure 3:** Violin plots of CH₄ diffusive (a) and total fluxes (b) during the studied period. Panel (c) depicts differences in the
 227 percentage contribution of diffusive to total fluxes. Solid lines are medians, while dashed lines denote quartiles. Asterisks
 228 indicate significant differences (* p<0.05, ** p<0.01, *** p<0.001, **** p<0.0001) between sampling dates determined by
 229 two-way ANOVA with Tukey's multiple comparison test. Note that a log scale is used here for clarity.

230

231 The total CH₄ fluxes show spatial variability within the fishpond that range four orders of magnitude (Fig. 3, 4;
 232 Suppl. Fig. 11; Suppl. Table 1). The observed spatial pattern showed high temporal variability on both daily and
 233 monthly scales (Fig. 2, 4, Suppl. Table 1). Most of the variability in CH₄ diffusive fluxes was explained by
 234 sampling date (62.4 %), while for the total CH₄ fluxes, spatial heterogeneity accounted for 87.2 % of data
 235 variability (Table 2). Using linear mixed-effects models, we identified water depth as the only significant predictor
 236 of total CH₄ fluxes (Df = 1, p < 0.0001, marginal Nakagawa's R² = 0.348; Fig. 5).

237

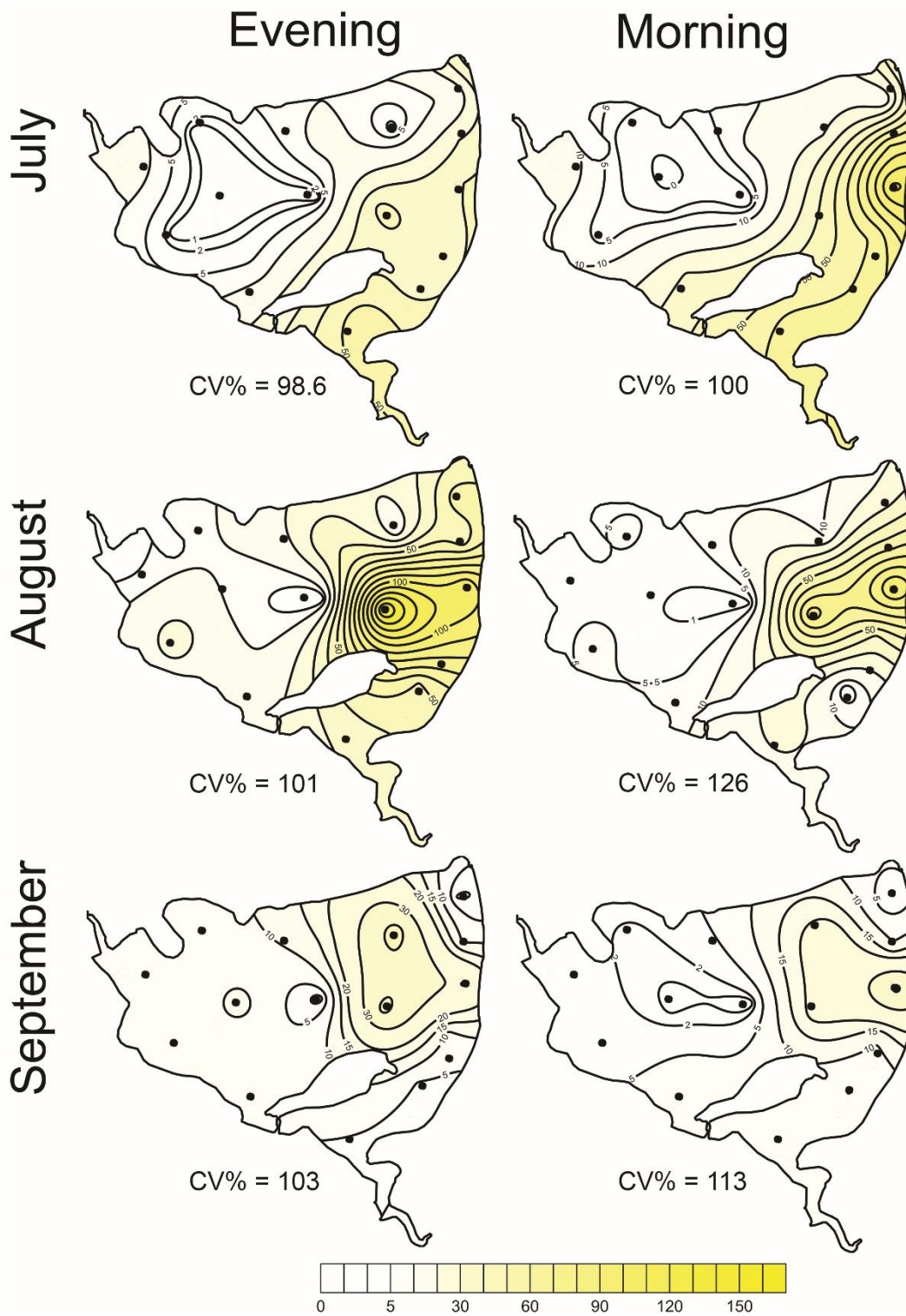
238

239

240 **Table 2:** The percentage of data variability explained by different factors (daytime, month = sampling date, and site)
 241 calculated with the Two-way RM ANOVA. Statistically significant values ($p < 0.01$) are bold.

	% of variability				Significance		
	Daytime	Month	Site	Unexplained	Daytime	Month	Site
CH₄ diffusive flux	2.3	62.4	13.2	22.1	0.0123	<0.0001	<i>n.s.</i>
CH₄ total flux	0.19	2.4	87.2	10.2	<i>n.s.</i>	<i>n.s.</i>	<0.0001
pH	4.4	64.9	11.1	19.6	0.0001	<0.0001	<i>n.s.</i>
Water temperature	3.3	92.3	2.5	1.9	<0.0001	<0.0001	<0.0001
O₂	21.7	48.1	13.8	16.4	<0.0001	<0.0001	0.0135
Chl-<i>a</i>	0.019	74.9	16.7	8.4	<i>n.s.</i>	<0.0001	<0.0001

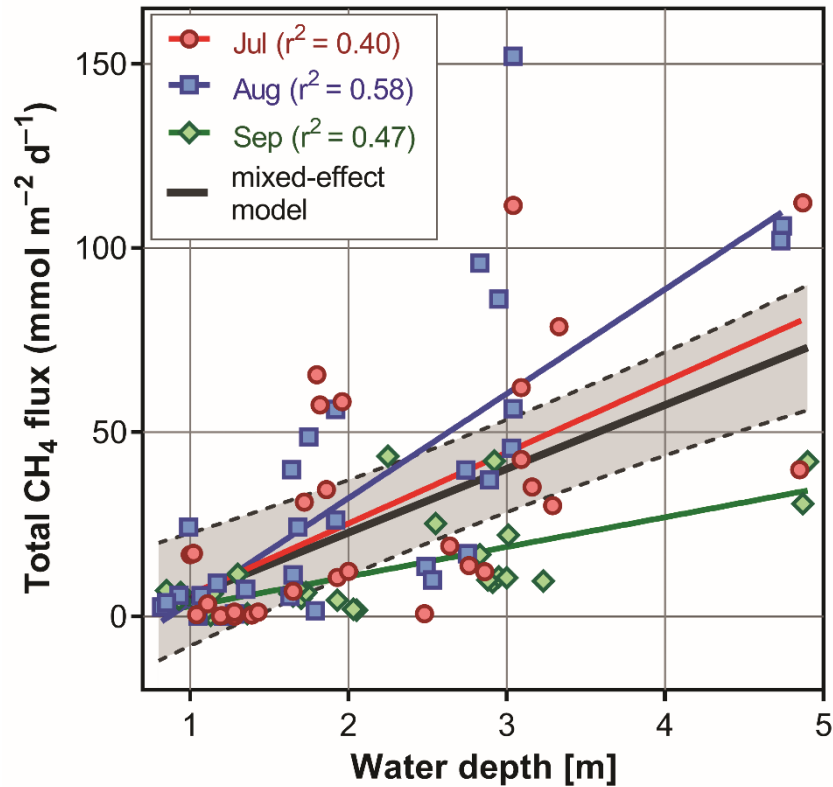
242 Interestingly, slopes of the linear regressions differed significantly among individual sampling campaigns (Fig. 5),
 243 indicating an additional season-related factor that affects CH₄ fluxes in the fishpond. Calculated CH₄ diffusive
 244 fluxes were not correlated with total fluxes. Linear mixed-effects models did not identify any significant predictor
 245 of the fluxes, indicating that factors and processes out of the study's scope are involved. We found no significant
 246 difference in either diffusive or total CH₄ fluxes between day and night.



247

248 **Figure 4:** Contour graphs of methane total fluxes in the Dehtář fishpond. Isopleths connect sites with the same value of
 249 methane fluxes ($\text{mmol m}^{-2} \text{ day}^{-1}$). CV% is a measure of spatial heterogeneity. Black dots representing the sampling sites.

250

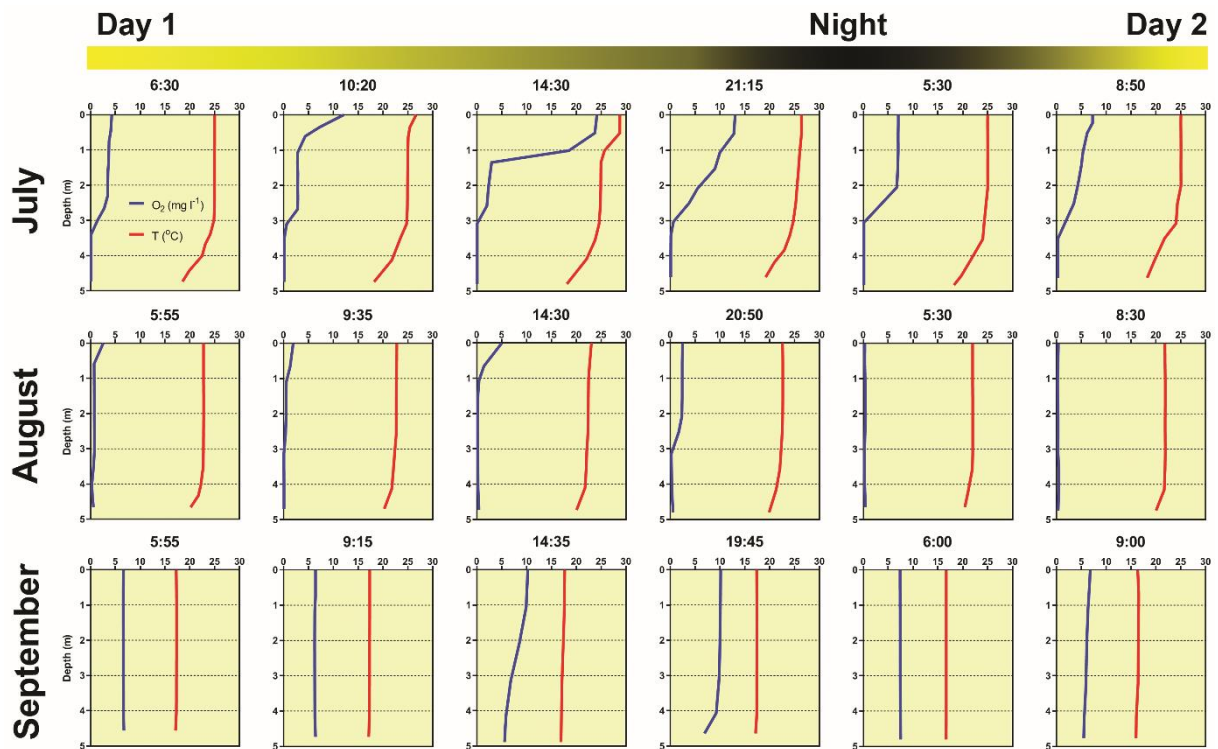


251

252 **Figure 5:** The most parsimonious linear mixed-effect model of methane total fluxes showing the water depth as the only
 253 significant predictor. Symbols are the measured values, the solid black line is the prediction, and dashed lines are 95th
 254 confidence intervals. Colours indicate month specific relation between total methane fluxes and water depth. Differences in
 255 slopes were tested using the F-test. In September, the slope of the regression line was significantly different from that in July
 256 and August.

257 3.3 Diurnal changes in vertical profiles of oxygen and temperature

258 Several contrasting patterns of vertical temperature and oxygen profiles occurred during summer 2019. Diurnal
 259 changes were most pronounced in July (Fig. 6). Surface temperatures varied from 25 °C in the morning to nearly
 260 30 °C in the afternoon. Thermal stratification of the water column was weak in the morning but became strongest
 261 at 14:30 with a thermocline at 0.5 m depth (Fig. 6). Later in the afternoon, the water column began to be mixed by
 262 wind. The morning vertical oxygen profile was characterised by a surface value of 4.3 mg L⁻¹, corresponding to
 263 51 % saturation and anoxia below 3 m.



264

265 **Figure 6:** Diurnal changes in vertical profiles of temperature and oxygen concentration measured at the deepest point of the
 266 fishpond. Numbers above each graph indicate the time of measurement.

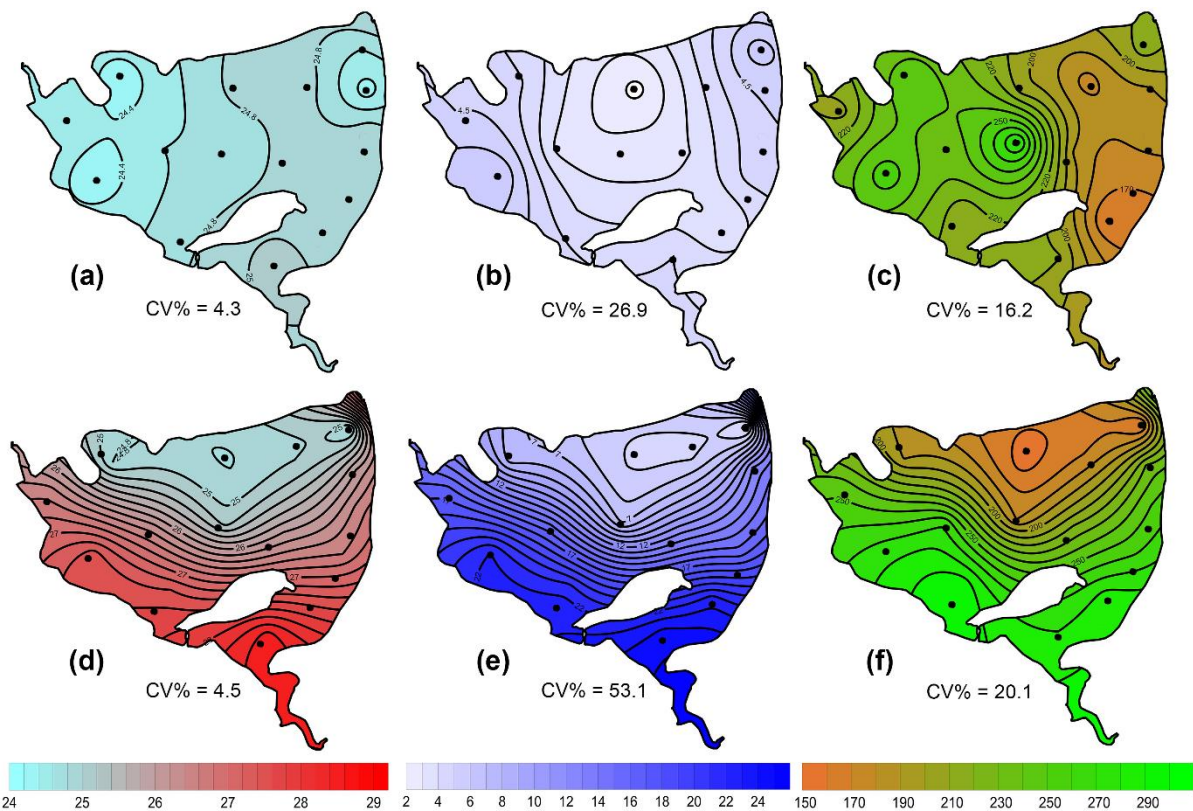
267 Due to the high photosynthetic activity of cyanobacteria, the surface oxygen concentration increased to 24 mg L^{-1}
 268 1 (320 % saturation, Fig. 6), and a steep oxycline was established at a depth of 0.5–1.5 m with no effect on the
 269 anoxic conditions at the deeper layers. Wind action eroded both the oxy- and thermoclines in the evening, and by
 270 the next morning, the vertical profiles were similar to those at the beginning.

271 In August, the water column was almost entirely mixed and low in oxygen in the morning, with only 2.6 mg L^{-1}
 272 (30 % saturation) of oxygen at the surface. Due to cloudy weather, the daily photosynthetic activity of
 273 phytoplankton resulted in only a slight increase in oxygen concentration at 0–1.5 m depth (4 mg L^{-1} , 47 %
 274 saturation). By the morning of the next day, the entire water column turned very close to anoxic (0.4 mg L^{-1} , 4 %
 275 saturation; Fig. 6), which in turn affected the spatial distribution of zooplankton, as evidenced by the formation of
 276 dense zooplankton clouds accumulated in the thin layer just at the surface (see Suppl. Fig. 3). In September, the
 277 water column was completely mixed, and we observed only weak daily changes in thermal and oxygen vertical
 278 structures (Fig. 6).

279 3.4 Effect of wind on spatial heterogeneity of temperature, oxygen and chlorophyll-*a*

280 During the summer, all measured parameters showed remarkable within-lake spatial heterogeneity (Suppl. Fig. 5–
 281 8). In July, meteorological conditions allowed for demonstrating the effect of wind on fishpond spatial

282 heterogeneity. In the morning, there were no substantial differences in the surface temperature and oxygen
 283 concentrations (Fig. 7ab). Phytoplankton biomass was accumulated mostly in the shallow western part, with the
 284 maximum in the centre (Fig. 7c). At 14:00, a light breeze started to blow from the northwest, achieving a maximum
 285 of 3.2 m s^{-1} (Suppl. Fig. 9). This episode lasted till the evening measurement, and the wind ceased by 21:00. The
 286 wind was strong enough to change spatial distribution substantially (Fig. 7d–f, Suppl. Fig. 4). In the evening, the
 287 surface water temperature on the windward (south) side of the fishpond was $\sim 4 \text{ }^\circ\text{C}$ higher than in the north (Fig.
 288 7d). The wind also induced order of magnitude differences in oxygen concentration along the north-south axis of
 289 the fishpond (3 mg L^{-1} of O_2 at the north, 24 mg L^{-1} of O_2 at the south; Fig. 7e) and affected phytoplankton
 290 distribution in the fishpond, resulting in remarkable bloom accumulation in the south (Fig. 7f, Suppl. Fig. 8).
 291 During the calm night after the disturbance, the north-south gradient substantially weakened. In August and
 292 September, the thermal heterogeneity of the pond was rather low, but the spatial distribution of oxygen and
 293 chlorophyll-*a* remained highly variable (Suppl. Fig. 5–8, Suppl. Table 1).



294
 295 **Figure 7:** Contour graphs of surface temperature (a, d; $^\circ\text{C}$), oxygen concentration (b, e; mg L^{-1}) and chlorophyll-*a*
 296 concentration (c, f; $\mu\text{g L}^{-1}$) measured on July 2 at different times of day: a, b and c are the morning measurements; d, e and f
 297 are evening measurements following a wind disturbance. Coefficient of variation (CV %) is a measure of spatial heterogeneity
 298 of measured parameters. Black dots representing the sampling sites.

299 **4 Discussion**

300 **4.1 Methane fluxes**

301 Assessing spatial heterogeneity of the CH₄ fluxes within a fishpond is critical for a reliable estimate of its
302 contribution to the global CH₄ budget. In our study, the variability in total CH₄ fluxes spanned several orders of
303 magnitude (ranging from 0.06 up to 1 121.3 mmol m⁻² d⁻¹), which is in agreement with similar studies (Casper et
304 al., 2000; DelSontro et al., 2016; Natchimuthu et al., 2016). However, most system-specific CH₄ flux estimates rely
305 on upscaling from a limited number of sites (Bastviken et al., 2004; Rasilo et al., 2015; Wik et al., 2016) because
306 obtaining spatial variability in CH₄ emission is methodologically challenging. In general, spatial heterogeneity
307 may reflect differences in water sources, physical mixing, local transformations and biogeochemical processes and
308 rates among lake habitats (Loken et al., 2019). In deep lakes, littoral areas can contribute disproportionately to
309 total lake CH₄ fluxes (Hofmann et al., 2010; Hofmann 2013, Natchimuthu et al., 2016; Schilder et al., 2013) and
310 are often missed by traditional sampling approaches (Wik et al., 2016). According to Wik et al. (2016), low
311 temporal and spatial resolutions are unlikely to cause overestimates. On the other hand, DelSontro et al. (2018b)
312 suggested that horizontal transport of CH₄ produced in littoral zones and the interaction between physical and
313 biological processes (e.g. air-water gas exchange, water column mixing, the interplay between CH₄ production
314 and microbial oxidation) may result in an underestimation of whole-lake CH₄ fluxes based on centre samples.
315 Similarly, Natchimuthu et al. (2016) found that up to 78 % underestimation would occur if samples obtained only
316 from the lake centre are used to extrapolate the total CH₄ flux. However, extrapolating our data from the deepest
317 point of the Dehtář fishpond would lead to an overestimation of the CH₄ fluxes by a factor of 2.9 (Suppl. Fig. 12).
318 The bias introduced by the deepest point measurement appears to be highly variable among systems with different
319 morphology, geographical location, mixing regimes or trophic states. For instance, analysis of 22 European lakes
320 during late summer has shown that spatially resolved CH₄ diffusive fluxes were highly variable for individual
321 lakes, yielding 55–300 % differences in the whole-lake estimates (Schilder et al., 2013). Schmiedeskamp et al.
322 (2021) observed an increase in CH₄ fluxes from the shore towards the centre in response to increasing sediment
323 C-content in two shallow German lakes. In line with these findings, our results provide further evidence that
324 spatially resolved data are needed to validate the uncertainties that come from using single-point samples to
325 represent whole-lake processes in hyper-eutrophic systems. As stated by Loken et al. (2019), rather than assuming
326 spatial homogeneity, scaling-up exercises of global carbon budgets should acknowledge the uncertainty that comes
327 from extrapolating from spatially limited data sets.

328 In the Dehtář fishpond, the total CH₄ fluxes increased with water depth, and this relationship was month specific.
329 The highest CH₄ fluxes at the deepest points may seem contradictory to previous studies, in which the highest
330 fluxes were typically observed in littoral areas (e.g., DelSontro et al., 2018b; Hofman et al., 2010; Natchimuthu et
331 al., 2016; Schilder et al., 2013). However, these findings are based on studying mostly large, shallow to medium-
332 deep oligotrophic lakes whose morphology, trophic state or oxygen regime sharply contrast with the hyper-
333 eutrophic Dehtář fishpond, where the upper two meters of the water column were oxygen-saturated while the
334 deepest strata were mostly anoxic, i.e., the extent and duration of bottom anoxia could be the most influential
335 factor contributing to the highest methane fluxes at the deepest point of the pond. In hyper-eutrophic systems, high
336 nutrient loading increases autochthonous primary production (Potužák et al., 2007; Rutegwa et al., 2019) and
337 promotes oxygen consumption and anaerobic decomposition in the sediments (Baxa et al., 2020), leading to
338 enhanced CH₄ production (Bastviken et al., 2004; Grasset et al., 2018). In aquaculture ponds in Southeast China,
339 CH₄ fluxes exhibited considerable spatial variations and peaked in the relatively deep feeding zone, where the
340 large loads of sediment organic matter fuelled CH₄ production (Yang et al., 2020). Furthermore, sediment
341 temperature was the strongest predictor of CH₄ fluxes in shallow ponds with anoxic hypolimnion (DelSontro et
342 al., 2016; Yang et al., 2020). It is, therefore, reasonable to assume that both temperature and oxygen concentration
343 in the sediment likely contributed to changes in observed CH₄ fluxes during the studied period in our study.
344 Although both parameters were not directly measured in the sediment, it can be deduced from their vertical profiles
345 that the probability of sediment anoxia was highest in August and lowest in September, and the sediment
346 temperature was lowest in September (see Fig. 5).

347 Our results agree with the generally accepted view that processes other than diffusive fluxes, most likely ebullition,
348 represent the major CH₄ pathway to the atmosphere in hyper-eutrophic ponds used for intensive fish production
349 (Kosten et al., 2020). Although freshwaters with high primary production are more likely to have high CH₄
350 ebullition rates (DelSontro et al., 2016), the dominant role of ebullition was also found across lentic systems
351 differing in size, trophic status or geographical location (Aben et al., 2017). Ebullition accounted on average for
352 56 % of total CH₄ fluxes in northern ponds in Canada (DelSontro et al., 2016), 49 and 71 % in two different zones
353 of Lake Taihu (Xiao et al., 2017) and 48-83 % in three Swedish lakes (Natchimuthu et al., 2016; Jansen et al.,
354 2019). The highest contribution was found in the small hyper-eutrophic Priest Pot (UK), where ebullition
355 represented 96 % of the total CH₄ flux from the pond (Casper et al., 2000). Apparently, the contribution of
356 ebullition can vary among systems and will remain uncertain until measurement designs cover enough
357 spatiotemporal variability to yield representative values for the whole ecosystem.

358 In shallow water bodies, a semi-stable flux of microbubbles was suggested to account for a significant portion of
359 the total CH₄ flux (Prairie and del Giorgio, 2013). When CH₄ concentration in the water column is above a certain
360 threshold of microbubble density, these microbubbles likely aggregate, fuse, and escape to the atmosphere from
361 buoyancy (Prairie and del Giorgio, 2013). Even a small fluctuation in hydrostatic pressure (e.g., due to changes in
362 atmospheric pressure) or lake water level was shown to trigger enhanced CH₄ ebullition (Bastviken et al., 2004;
363 Casper et al., 2000; Varadharajan and Hemond, 2012). Since ebullition rates increase exponentially with
364 temperature, CH₄ fluxes tend to peak in warm summer months (van Bergen et al., 2019). In our study, 1 % lower
365 air pressure in July and August than in September, along with bottom anoxia and higher water temperature, could
366 account for the enhanced release of CH₄ bubbles from the sediment (31.7 mmol m⁻² d⁻¹, >90 % of total CH₄ fluxes;
367 Suppl. Fig. 2). In September, when we observed the lowest water temperatures from the studied period and the
368 oxygen profile was rather uniform, ebullition accounted for 81 % (11 mmol m⁻² d⁻¹) of the total CH₄ fluxes. The
369 spatially pooled data of the total CH₄ fluxes measured in the Dehtář fishpond varied from 11.8 to 34.5 mmol m⁻²
370 d⁻¹, which is comparable with similar systems elsewhere (e.g., Bastviken et al., 2010; van Bergen et al., 2019;
371 Baron et al., 2022). To sum up, both diffusive fluxes and ebullition must be addressed to understand the magnitude
372 of total aquatic CH₄ fluxes and how their relative contributions vary across and within aquatic systems (Kosten et
373 al., 2020). Moreover, with an improved determination of CH₄ hot-spots and its causes, the management of ponds
374 could be changed accordingly and so the overall emissions reduced for example by decreasing P-availability and
375 dredging (Nijman et al., 2022).

376 **4.2 Effect of wind event on ecosystem spatial structure**

377 Sudden changes in ecosystem spatial structure in response to meteorological forcing have rarely been documented
378 (Loken et al., 2019) since they are hard to predict. Research into them using traditional methods requires intensive
379 effort or expensive instrumentation (Ortiz and Wilkinson, 2021), and it remains a matter of luck to obtain a relevant
380 dataset. In the July sampling campaign, we observed a strong impact of the wind on environmental heterogeneity
381 in the fishpond, which was apparent at a sub-daily time scale. Due to the methodological constraints, i.e., lack of
382 initial measurement, we can only speculate about the effect of wind on the total CH₄ fluxes. The northwest wind
383 during the day advected warmed surface water with cyanobacterial bloom from the north basin to the south. In the
384 evening, it resulted in bloom accumulation on the upward side and a north-south gradient of more than 4 °C and
385 20 mg L⁻¹ oxygen. After the winds fell off, the observed gradients declined during cooling at night. We assume
386 that the wind blowing across the pond surface drove buoyant cyanobacteria and surface water downwind and
387 caused an upwelling of deeper, colder, and hypoxic water on the upwind side. This wind-related circulation pattern

388 has been described as a “conveyor belt” in classical textbooks (Reynolds et al., 2006), held responsible for a
389 disruption of the thermal structure of the water column and the non-uniform spatial distribution of pH, oxygen,
390 CO₂ or CH₄ and also plankton assemblages (e.g., Loken et al., 2019; Natchimuthu et al., 2016; Rinke et al., 2009;
391 Ortiz and Wilkinson, 2021).

392 Similar to our study, mild winds (~4 m s⁻¹) were strong enough to redistribute heat and induce lake-wide
393 circulations driving upwelling and downwelling in 24 m deep Lake Pleasant (Czikowsky et al., 2018). As the wind
394 blows harder and lasts longer, the effects on ecosystem functioning may target higher trophic levels and become
395 more complex (Rinke et al., 2009). In Lake Constance, a three-day storm event with wind velocities of ~10 m s⁻¹
396 resulted in a lake-wide displacement of water masses and the formation of the 6–15 °C horizontal surface water
397 gradient, which in turn changed the spatial distribution of phytoplankton, zooplankton and juvenile fish (Rinke et
398 al., 2009). After several stormy days (wind velocities of 12–15 m s⁻¹), Čech et al. (2011) observed negative effects
399 of wind-driven changes in water temperature and wave action on perch (*Perca fluviatilis*) spawning in the Lake
400 Milada. Although wind events affect shallow and deep lakes differently, there is growing evidence that they can
401 have far-reaching consequences on the functioning of aquatic ecosystems by disrupting energy flows, nutrient
402 fluxes, productivity and reproduction, and consequently altering community composition and trophic interactions
403 in the short and long term (Stockwell et al., 2020). As the frequency, intensity, spatial extent and duration of these
404 extreme meteorological events are projected to increase due to ongoing climate change (Comou and Rahmstorf,
405 2012), there is an urgent need to better understand the mechanisms underlying their impacts on the maintenance
406 of the ecosystem services.

407 **4.3 Summer changes in the oxygen regime**

408 Our data demonstrate that shallow, hyper-eutrophic ponds have disrupted oxygen regimes (Baxa et al., 2021) with
409 anoxic hypolimnion and may experience severe whole-water column hypoxia critical for aquatic biota (Miranda
410 et al., 2001). The hypoxic periods may result, for example, from sudden weather change (Jeppesen et al., 1990)
411 and last several days, during which physical processes and phytoplankton photosynthesis cannot compensate for
412 intense community respiration (Baxa et al., 2021). This became obvious in August when severe oxygen depletion
413 was measured at the surface across the whole pond, mostly far below a critical level of 4.5 mg L⁻¹, when adverse
414 effects came into play (Banerjee et al., 2019). However, oxygen surface concentrations in shallow parts of the
415 pond were substantially higher regardless of the time of day, which contrasts with findings of Miranda et al. (2001),
416 who emphasised shallow waters as the most sensitive parts of lakes, where hypoxic events can occur due to the
417 respiration of sediment biota. The observed spatial gradients of oxygen may create temporal refugia which allow

418 fish to survive harsh conditions that occur in the deepest part of the pond. To minimise economic losses and
419 negative impacts on the ecosystem, future research should identify the interplay between meteorological forcing,
420 trophic status and anthropogenic pressures (e.g., management practices) that affect oxygen fluctuations at various
421 time scales.

422 **4.4 Study limitations**

423 Like in other research, there are some limitations in the current study. Since our measurement had only a limited
424 temporal resolution (three samplings during the summer season), it is not appropriate to extrapolate CH₄ emissions
425 for annual values. Noticeably, future research must increase the frequency of the sampling and include also
426 innovative techniques to measure CH₄ fluxes at multiple fishponds, with different management regime. In our
427 study, the 12-h deployment time of the floating chambers could have led to extensive gas accumulation, which in
428 turn might have resulted in an underestimation of the total CH₄ fluxes due to the dissolution of the CH₄ from the
429 chamber into the water once the equilibrium concentration in the chamber is overcome (Bastviken et al., 2010).
430 However, CH₄ concentrations in water corresponded to a supersaturation of several orders of magnitude, so the
431 introduced bias appears to be of minor importance. In any case, our daily spatially pooled total CH₄ fluxes (11.8–
432 34.5 mmol m⁻² d⁻¹) represent a rather conservative estimate for the global methane budget. In our study, we also
433 did not address the important processes that could shed light on the lake CH₄ budget, such as CH₄ oxidation rates
434 (Bastviken et al., 2008) or biological interaction (e.g., protistan grazing on CH₄ oxidising bacteria) in aquatic food
435 webs (Sanseverino et al., 2012) that can affect the overall CH₄ fluxes. We also lack information about spatial
436 differences in sediment microbiota and organic carbon content and compositions, which were found to affect CH₄
437 production rates (Berberich et al., 2020; Emerson et al., 2021). Despite the limitation mentioned above, our results
438 show that complementary spatial surveys help contextualise the fixed station dynamics and provide additional,
439 management-relevant information about the fishpond.

440 For improved monitoring strategies, however, a continuous measurement approach like eddy covariance would be
441 generally more efficient than traditional sampling at regular intervals. Eddy covariance accounts for temporal
442 variability and provides high temporal resolution data by continuously measuring wind speed, gas concentration,
443 and vertical turbulent fluxes to estimate methane emissions (Erkkilä et al., 2018). More importantly, it also offers
444 spatially integrated measurements, averaging emissions over a larger area and therefore accounts for pond spatial
445 heterogeneity. However, it's worth noting that the choice of monitoring approach depends on various factors,
446 including the specific objectives, available resources, and the characteristics of the emission sources. To accurately
447 capture both short-term variability and lake spatial heterogeneity of methane ebullition and diffusion fluxes, the

448 most efficient approach was found to be a combination of continuous measurements with traditional methods
449 including floating chambers, anchored funnels and boundary model calculations (Schubert et al., 2012; Podgrajsek
450 et al., 2014; Erkkilä et al., 2018). This integrated approach would provide a comprehensive understanding of
451 methane emissions, enabling better estimation and more effective mitigation efforts.

452 **5 Conclusions**

453 Many fishponds are hundreds of years old (Potužák et al., 2007), and as such, they are an integral part of our
454 cultural heritage. Nowadays, ponds face a variety of conflicting interests often leading to a focus on maximising
455 fish production that comes at the expense of other ecological services. Intensification of fish production has
456 brought a transition from the traditional management based on natural processes to practices involving
457 supplementary feeding, fertilisation, and overstocking (Pechar, 2000). These changes coupled with the impacts of
458 climate change has resulted to frequent anoxic events and cyanobacterial blooms that reduce biodiversity and limit
459 recreational activities increasingly valued by the public. Our study not only illustrates common water quality
460 problems in fishponds but also provides compelling evidence that methane emissions in these degraded ecosystems
461 further exacerbates negative climate feedbacks and should be considered in discussions to advance the
462 development of sustainable management.

463 Deciphering the mechanisms that drive spatial and temporal heterogeneity in aquatic ecosystem structure and
464 function not only expands our understanding of pond ecology but also provides insights to improve the
465 management of these ecosystems and the services they provide. Our results suggest that spatial heterogeneity needs
466 to be considered when designing experiments and monitoring programs. Without the spatially resolved sampling,
467 we introduce bias into our datasets, hampering our limnological understanding of the ecosystem's functioning and
468 impeding our ability to accurately estimate rates such as methane emissions on a global scale (DeI Sontro et al.,
469 2018a). In agreement with Kosten et al. (2020), we demonstrated that neglecting ebullition leads to a considerable
470 underestimating of the total CH₄ fluxes. Since there are thousands of these intensively managed fishponds, we
471 argue for changing the management practices toward sustainable use of natural resources to mitigate the overall
472 emissions of greenhouse gases from these ecosystems. Future studies are needed to characterise CH₄ fluxes over
473 a greater number and diversity of aquaculture ponds and examine the mechanisms controlling CH₄ emissions in
474 aquatic ecosystems.

475 **Acknowledgements**

476 The study was supported by the Czech Science Foundation (Research Projects No. 17-09310S, 19-23261S and
477 P504/19-16554S). We thank Martin Rulík for providing us gas chambers. We especially thank to Miloslav Šimek
478 and Linda Jiřová for enabling gas analyses. We are grateful Anna Sieczko for consultation on the calculation of
479 CH₄ fluxes. English correction was made by Anton Baer.

480 **Data availability**

481 Dataset associated with the manuscript can be found in the GitHub Repositories under
482 <https://zenodo.org/badge/latestdoi/587640213>.

483 **Author contributions**

484 All authors contributed to the study conception and design. PZ planned the campaign; PZ, AM and JN performed
485 the sampling and analyzed the data; AM performed the gas-measurements; VK performed statistical analyses and
486 modelling; PZ and AM wrote the manuscript. All authors read and approved the final manuscript.

487 **References**

- 488 Aben, R.C.H., Barros, N., van Donk, E., Frenken, T., Hilt, S., Kazanjian, G., Lamers, L.P.M., Peeters, E.T.H.M.,
489 Roelofs, J.G. M, de Senerpont Domis, L.N., Stephan, S., Velthuis, M., Van de Waal, D.B., Wik, M., Thornton,
490 B.F., Wilkinson, J., DelSontro, T., and Kosten, S.: Cross continental increase in methane ebullition under climate
491 change. *Nat. Commun.*, 8, 1682, <https://doi.org/10.1038/s41467-017-01535-y>, 2017.
- 492 Banerjee, A., Chakrabarty, M., Rakshit, N., Bhowmick, A.R., and Ray, S.: Environmental factors as indicators of
493 dissolved oxygen concentration and zooplankton abundance: deep learning versus traditional regression approach.
494 *Ecol. Indic.*, 100, 99-117, <https://doi.org/10.1016/j.ecolind.2018.09.051>, 2019.
- 495 Baron, A.A.P., Dyck, L.T., Amjad, H., Bragg, J., Kroft, E., Newson, J., Oleson, K., Casson, N.J., North, R.L.,
496 Venkiteswaran, J.J., and Whitfield, C.J.: Differences in ebullitive methane release from small, shallow ponds
497 present challenges for scaling. *Sci. Total Environ.*, 802, 149685, <https://doi.org/10.1016/j.scitotenv.2021.149685>,
498 2022.
- 499 Bartosiewicz, M., Maranger, R., Przytulska, A., and Laurion, I.: Effects of phytoplankton blooms on fluxes and
500 emissions of greenhouse gases in a eutrophic lake. *Water Res.*, 196, 116985,
501 <https://doi.org/10.1016/j.watres.2021.116985>, 2021.
- 502 Bastviken, D., Cole, J., Pace M., and Tranvik, L.: Methane emissions from lakes: Dependence of lake
503 characteristics, two regional assessments, and a global estimate. *Global Biogeochem. Cycles*, 18, GB4009,
504 <https://doi.org/10.1029/2004GB002238>, 2004.

505 Bastviken, D., Cole, J.J., Pace, M.L., and Van de Bogert, M.C.: Fates of methane from different lake habitats:
506 connecting whole-lake budgets and CH₄ emissions. *J. Geophys. Res. Biogeosci.*, 113, G02024,
507 <https://doi.org/10.1029/2007JG000608>, 2008.

508 Bastviken, D., Santoro, A.L., Marotta, H., Pinho, L.Q., Calheiros, D.F., Crill, P., and Enrich-Prast, A.: Methane
509 Emissions from Pantanal, South America, during the Low Water Season: Toward More Comprehensive Sampling.
510 *Environ. Sci. Tech.*, 44, 5450-5455, <https://doi.org/10.1021/es1005048>, 2010.

511 Bates, D., Maechler, M., Bolker, B., and Walker, S.: Fitting Linear Mixed-Effects Models Using lme4. *J. Stat.*
512 *Soft.*, 67, 1-48, <https://doi.org/10.18637/jss.v067.i01>, 2015.

513 Baxa, M., Musil, M., Kummel, M., Hazlík, O., Tesařová, B., and Pechar, L.: Dissolved oxygen deficits in a shallow
514 eutrophic aquatic ecosystem (fishpond) – Sediment oxygen demand and water column respiration alternately drive
515 the oxygen regime. *Sci. Total Environ.*, 766, 142647, <https://doi.org/10.1016/j.scitotenv.2020.142647>, 2021.

516 Berberich, M.E., Beaulieu, J.J., Hamilton, T.L., Waldo, S., and Buffam, I.: Spatial variability of sediment methane
517 production and methanogen communities within a eutrophic reservoir: Importance of organic matter source and
518 quantity. *Limnol. Oceanogr.*, 65, 1336-1358, <https://doi.org/10.1002/lno.11392>, 2020.

519 Bižić, M., Klintzsch, T., Ionescu, D., Hindiyeh, M.Y., Günthel, M., Muro-Pastor, A.M., Eckert, W., Urich, T.,
520 Keppler, F., and Grossart, H.P.: Aquatic and terrestrial cyanobacteria produce methane. *Sci. Adv.*, 6, 1-10,
521 <https://doi.org/10.1126/sciadv.aax5343>, 2020.

522 Bussmann, I., Matoušů, A., Osudar, R., and Mau, S.: Assessment of the radio ³H-CH₄ tracer technique to measure
523 aerobic methane oxidation in the water column. *Limnol. Oceanogr.- Meth.*, 13, 312-327,
524 <https://doi.org/10.1002/lom3.10027>, 2015.

525 Casper, P., Maberly, S.C., Hall, G.H., and Finlay, B.J.: Fluxes of methane and carbon dioxide from a small
526 productive lake to the atmosphere. *Biogeochemistry*, 49, 1-19, <https://doi.org/10.1023/A:1006269900174>, 2000.

527 Čech, M., Peterka, J., Říha, M., Muška, M., Hejzlar, J., and Kubečka, J.: Location and timing of the deposition of
528 eggs strands by perch (*Perca fluviatilis* L.): the roles of lake hydrology, spawning substrate and female size.
529 *Knowl. Manag. Aquat. Ecosyst.*, 403, 1-12, <https://doi.org/10.1051/kmae/2011070>, 2011.

530 Céréghino, R., Biggs, J., Oertli, B., and Declerck, S.: The ecology of European ponds: defining the characteristics
531 of a neglected freshwater habitat. *Hydrobiologia*, 597, 1-6, <https://doi.org/10.1007/s10750-007-9225-8>, 2008.

532 Coumou, D. and Rahmstorf, S.: A decade of weather extreme. *Nat. Clim. Change*, 2, 491-96,
533 <https://doi.org/10.1038/nclimate1452>, 2012.

534 Crusius, J. and Wanninkhof, R.: Gas transfer velocities measured at low wind speed over a lake. *Limnol. Oceanogr.*,
535 48, 1010-1017, <https://doi.org/10.4319/lo.2003.48.3.1010>, 2003.

536 Czikowsky, M.J., MacIntyre, S., Tedford, E.W., Vidal, J., and Miller, S.D.: Effects of wind and buoyancy on
537 carbon dioxide distribution and air-water flux of a stratified temperate lake. *J. Geophys. Res. Biogeosci.*, 123,
538 2305-2322, <https://doi.org/10.1029/2017JG004209>, 2018.

539 De Meester, L., Declerck, S., Stoks, R., Louette, G., Van de Meutter, F., De Bie, T., Michels, E., and Brendonck,
540 L.: Ponds and pools as model systems in conservation biology, ecology and evolutionary biology. *Aquat. Cons.*,
541 15, 715-725, <https://doi.org/10.1002/aqc.748>, 2005.

542 DelSontro, T., Boutet, L., St-Pierre, A., del Giorgio, P.A., and Prairie, Y.T.: Methane ebullition and diffusion from
543 northern ponds and lakes regulated by the interaction between temperature and system productivity. *Limnol.*
544 *Oceanogr.*, 61, 62-77, <https://doi.org/10.1002/lno.10335>, 2016.

545 DelSontro, T., Beaulieu, J.J., and Downing, J.J.: Greenhouse gas emissions from lakes and impoundments:
546 upscaling in the face of global change. *Limnol. Oceanogr. Lett.*, 3, 64-75, <https://doi.org/10.1002/lol2.10073>,
547 2018a.

548 DelSontro, T., del Giorgio, P.A., and Prairie, Y.T.: No Longer a Paradox: The Interaction Between Physical
549 Transport and Biological Processes Explains the Spatial Distribution of Surface Water Methane Within and Across
550 Lakes. *Ecosystems*, 21, 1073-1087, [10.1007/s10021-017-0205-1](https://doi.org/10.1007/s10021-017-0205-1), 2018b.

551 Emerson, J.B., Varner, R.K., Wik, M., Parks, D.H., Neumann, R.B., Johnson, J.E., Singleton, C. M., Woodcroft,
552 B.J., Tollerson II, R., Owusu-Domney, A., Binder, M., Freitas, N. L., Crill, P.M., Saleska, S.R., Tyson, G.W., and
553 Rich, V.I.: Diverse sediment microbiota shape methane emission temperature sensitivity in Arctic lakes. *Nat.*
554 *Commun.*, 12, 5815, <https://doi.org/10.1038/s41467-021-25983-9>, 2021.

555 Erkkilä, K.-M., Ojala, A., Bastviken, D., Biermann, T., Heiskanen, J. J., Lindroth, A., Peltola, O., Rantakari, M.,
556 Vesala, T., and Mammarella, I.: Methane and carbon dioxide fluxes over a lake: comparison between eddy
557 covariance, floating chambers and boundary layer method, *Biogeosciences*, 15, 429–445,
558 <https://doi.org/10.5194/bg-15-429-2018>, 2018.

559 Grasset, Ch., Mendonça, R., Saucedo, G.V., Bastviken, D., Roland, F., and Sobek, S.: Large but variable methane
560 production in anoxic freshwater sediment upon addition of allochthonous and autochthonous organic matter.
561 *Limnol. Oceanogr.*, 63, 1488-1501, <https://doi.org/10.1002/lno.10786>, 2018.

562 Halekoh, H. and Hojsgaard, S.: A Kenward-Roger Approximation and Parametric Bootstrap Methods for Tests in
563 Linear Mixed Models - The R Package pbrtest. *J. Stat. Soft.*, 59, 1-30, <https://doi.org/10.18637/jss.v059.i09> 2014.

564 Hofmann, H., Federwisch, L., and Peeters, F.: Wave-induced release of methane: littoral zones as a source of
565 methane in lakes. *Limnol. Oceanogr.*, 55, 1990-2000, <https://doi.org/10.4319/lo.2010.55.5.1990>, 2010.

566 Hofmann, H.: Spatiotemporal distribution patterns of dissolved methane in lakes: How accurate are the current
567 estimations of the diffusive flux path? *Geophys. Res. Lett.*, 40, 2779-2784, <https://doi.org/10.1002/grl.50453>,
568 2013.

569 Hu, Z., Wu, S., Ji, Ch., Zou, J., Zhou, Q., and Liu, S.: A comparison of methane emissions following rice paddies
570 conversion to crab-fish farming wetlands in southeast China. *Environ. Sci. Pollut. Res.*, 23, 1505-1515,
571 <https://doi.org/10.1007/s11356-015-5383-9>, 2016.

572 Jansen, J., Thornton, B.F., Jammot, M.M., Wik, M., Cortés, A., Friborg, T., MacIntyre, S., and Crill, P.M.:
573 Climate-sensitive controls on large spring emissions of CH₄ and CO₂ from northern lakes. *J. Geophys. Res.*,
574 *Biogeosciences*, 124, 2379-2399, <https://doi.org/10.1029/2019JG005094>, 2019.

575 Jähne, B., Münnich, K. O., Börsinger, R., Dutzi, A., Huber, W., and Libner, P.: On the parameters influencing air-
576 water gas exchange, *J. Geophys. Res.*, 92, C2, 1937-1949, doi:10.1029/JC092iC02p01937, 1987.

577 Jeppesen, E., Søndergaard, M., Sortkjaer, O., Mortensen, E., and Kristensen, P.: Interactions between
578 phytoplankton zooplankton and fish in a shallow hypertrophic Lake a study of phytoplankton collapses in Lake
579 Sobygaard, Denmark. *Hydrobiologia*, 1991, 149-164, <https://doi.org/10.1007/BF00026049>, 1990.

580 Kolar, V., Vlašánek, P., and Boukal, D.S.: The influence of successional stage on local odonate communities in
581 man-made standing waters. *Ecol. Eng.*, 173, 106440, <https://doi.org/10.1016/j.ecoleng.2021.106440>, 2021.

582 Kopáček, J. and Hejzlar, J.: Semi-micro determination of total phosphorus in fresh waters with perchloric acid
583 digestion. *Int. J. Environ. Anal. Chem.*, 53, 173-183, <https://doi.org/10.1080/03067319308045987>, 1993.

584 Kopáček, J. and Procházková, L.: Semi-Micro Determination of Ammonia in Water by the Rubazoic Acid Method.
585 *Int. J. Environ. Anal. Chem.*, 53, 243-248, <https://doi.org/10.1080/03067319308045993>, 1993.

586 Kosten, S., Almeida, R.M., Barbosa, I., Mendonça, R., Muzitano, I.S., Oliveira-Junior, E.S., Vroom, R.J.E., Wang,
587 H.J., and Barros, N.: Better assessments of greenhouse gas emissions from global fish ponds needed to adequately
588 evaluate aquaculture footprint. *Sci. Total Environ.*, 748, 141247, <https://doi.org/10.1016/j.scitotenv.2020.141247>,
589 2020.

590 Laas, A., Noges, P., Koiv, T., and Noges, T.: High-frequency metabolism study in a large and shallow temperate
591 lake reveals seasonal switching between net autotrophy and net heterotrophy. *Hydrobiologia*, 694, 57-74,
592 <https://doi.org/10.1007/s10750-012-1131-z>, 2012.

593 Loken, L.C., Crawford, J.T., Schramm, P.J., Stadler, P., Desai, A.R., and Stanley, E.H.: Large spatial and temporal
594 variability of carbon dioxide and methane in a eutrophic lake. *J. Geophys. Res. Biogeosci.*, 124, 2248-2266
595 <https://doi.org/10.1029/2019JG005186>, 2019.

596 Lüdecke, D.: “ggeffects: Tidy Data Frames of Marginal Effects from Regression Models.” *J. Open Source Soft.*,
597 3, 772, <https://doi.org/10.21105/joss.00772>, 2018.

598 Lüdecke, D., Makowski, D., and Waggoner, P.: performance: Assessment of Regression Models Performance. R
599 package version 0.4.4. <https://CRAN.R-project.org/package=performance>, 2020.

600 Ma, Y., Sun, L., Liu, C., Yang, X., Zhou, W., Yang, B., Schwenke, G., and Liu, D.L.: A comparison of methane
601 and nitrous oxide emissions from inland mixed-fish and crab aquaculture ponds. *Sci. Total Environ.*, 637-638,
602 517-523, <https://doi.org/10.1016/j.scitotenv.2018.05.040>, 2018

603 McAuliffe, C.: Gas Chromatographic determination of solutes by multiple phase equilibrium. *Chem. Technol.*, 1,
604 46-51, 1971.

605 Miranda, L.E., Hargreaves, J.A., and Raborn, S.W.: Predicting and managing risk of unsuitable dissolved oxygen
606 in a eutrophic lake. *Hydrobiologia*, 457, 177-185, <https://doi.org/10.1023/A:1012283603339>, 2001.

607 Murphy, J. and Riley, J.P.: A modified single-solution method for the determination of phosphate in natural waters.
608 *Anal. Chim. Acta*, 27, 31-36, [https://doi.org/10.1016/S0003-2670\(00\)88444-5](https://doi.org/10.1016/S0003-2670(00)88444-5), 1962.

609 Natchimuthu, S., Sundgren, I., Gålfalk, M., Klemetsson, L., Crill, P., Danielsson, Å., and Bastviken, D.: Spatio-
610 temporal variability of lake CH₄ fluxes and its influence on annual whole lake emission estimates. *Limnol.*
611 *Oceanogr.*, 61, 13-26, <https://doi.org/10.1002/lno.10222>, 2016.

612 Nijman, T.P.A., Lemmens, M., Lurling, M., Kosten, S., Welte, C., and Veraart, A.J.: Phosphorus control and
613 dredging decrease methane emissions from shallow lakes. *Sci. Total Environ.*, 847, 15758,
614 <https://doi.org/10.1016/j.scitotenv.2022.157584>, 2022.

615 Ortiz, D.A. and Wilkinson, G.M.: Capturing the spatial variability of algal bloom development in a shallow
616 temperate lake. *Freshwater Biol.*, 66, 2064-2075, <https://doi.org/10.1111/fwb.13814>, 2021.

617 Pechar, L.: Impacts of long-term changes in fishery management on the trophic level and water quality in Czech
618 fishponds. *Fisheries Manag. Ecol.*, 7, 23-32, [10.1046/j.1365-2400.2000.00193.x](https://doi.org/10.1046/j.1365-2400.2000.00193.x), 2000.

619 Pokorný, J. and Hauser, V.: The restoration of fish ponds in agricultural landscapes. *Ecol. Eng.*, 18, 555-574,
620 [https://doi.org/10.1016/S0925-8574\(02\)00020-4](https://doi.org/10.1016/S0925-8574(02)00020-4), 2002.

621 Podgrajsek, E., Sahlée, E., Bastviken, D., Holst, J., Lindroth, A., Tranvik, L., and Rutgersson, A.: Comparison of
622 floating chamber and eddy covariance measurements of lake greenhouse gas fluxes, *Biogeosciences*, 11, 4225–
623 4233, <https://doi.org/10.5194/bg-11-4225-2014>, 2014.

624 Potužák, J., Hůda, J., and Pechar, L.: Changes in fish production effectivity in eutrophic fishponds – impact of
625 zooplankton structure. *Aquacult. Int.*, 15, 201-210, <https://doi.org/10.1007/s10499-007-9085-2>, 2007.

626 Potužák, J., Duras, J., and Drozd, B.: Mass balance of fishponds: are they sources or sinks of phosphorus?
627 *Aquacult. Int.*, 24, 1725-1745, <https://doi.org/10.1007/s10499-016-0071-4>, 2016.

628 Prairie, Y.T. and del Giorgio, P.A.: A new pathway of freshwater methane emissions and the putative importance
629 of microbubbles. *Inland Waters*, 3, 311-320, <https://doi.org/10.5268/IW-3.3.542>, 2013.

630 Procházková, L.: Bestimmung der Nitrate im Wasser. *Zeitschrift für Analytische Chemie*, 167, 254-260, 1959.

631 Rasilo, T., Prairie, Y.T., and del Giorgio, P.A.: Large-scale patterns in summer diffusive CH₄ fluxes across boreal
632 lakes, and contribution to diffusive C emissions. *Glob. Change Biol.*, 21, 1124-1139,
633 <https://doi.org/10.1111/gcb.12741>, 2015.

634 R Core Team: A language and environment for statistical computing. R Foundation for Statistical Computing.
635 Vienna, Austria <https://www.R-project.org/>, 2018.

636 Reynolds, C.S.: Ecology of phytoplankton, Cambridge University Press, Cambridge,
637 <https://doi.org/10.1017/CBO9780511542145>, 2006.

638 Rinke, K., Huber, A.M.R., Kempke, S., Eder, M., Wolf, T., Probst, W.N., and Rothhaupt, K.: Lake-wide
639 distributions of temperature, phytoplankton, zooplankton, and fish in the pelagic zone of a large lake. *Limnol.*
640 *Oceanogr.*, 54, 1306-1322, <https://doi.org/10.4319/lo.2009.54.4.1306>, 2009.

641 Rutegwa, M., Potužák, J., Hejzlar, J., and Drozd, B.: Carbon metabolism and nutrient balance in a hypereutrophic
642 semi-intensive fishpond. *Knowl.Manag. Aquat. Ecosyst.*, 49, <https://doi.org/10.1051/kmae/2019043>, 2019.

643 Sanseverino, A.M., Bastviken, D., Sundh, I., Pickova, J., and Enrich-Prast, A.: Methane carbon supports aquatic
644 food webs to the fish level. *PLoS One*7, e42723, <https://doi.org/10.1371/journal.pone.0042723>, 2012.

645 Scheffer, M.: Ecology of shallow lakes. Population and Community Biology Series. Springer, 357 p.,
646 <https://doi.org/10.1007/978-1-4020-3154-0>, 2004.

647 Schilder, J., Bastviken, D., van Hardenbroek, M., Kankaala, P., Rinta, P., Stötter, T., and Heiri, O.: Spatial
648 heterogeneity and lake morphology affect diffusive greenhouse gas emission estimates of lakes. *Geophys. Res.*
649 *Lett.*, 40, 5752-5756, <https://doi.org/10.1002/2013GL057669>, 2013.

650 Schmiedeskamp, M., Praetzel, L.S.E., Bastviken, D., and Knorr, K.H.: Whole-lake methane emissions from two
651 temperate shallow lakes with fluctuating water levels: Relevance of spatiotemporal patterns. *Limnol. Oceanogr.*,
652 66, 2455-2469, <https://doi.org/10.1002/lno.11764>, 2021.

653 Schubert, C.J., Diem, T., Eugster W.: Methane emissions from a small wind shielded lake determined by eddy
654 covariance, flux chambers, anchored funnels, and boundary model calculations: a comparison. *Environ. Sci.*
655 *Technol.*, 46, 4515-4522, <https://doi.org/10.1021/es203465x>, 2012

656 Stanley, E.H., Collins, S.M., Lottig, N.R., Oliver, S.K., Webster, K.E., Cheruvilil, K.S., and Soranno, P.A.: Biases
657 in lake water quality sampling and implications for macroscale research. *Limnol. Oceanogr.*, 64, 1572-1585,
658 <https://doi.org/10.1002/lno.11136>, 2019.

659 Stockwell, J.D., Doubek, J.P., Adrian, R., Anneville, O., Carey, C.C., Carvalho, L., Domis, L.N.D.S., Dur, G.,
660 Frassl, M.A., Grossart, H.-P., Ibelings, B.W., Lajeunesse, M.J., Lewandowska, A.M., Llames, M.E., Matsuzaki,
661 S.-I.S., Nodine, E.R., Nöges, P., Patil, V.P., Pomati, F., Rinke, K., Rudstam, L.G., Rusak, J.A., Salmaso, N.,
662 Seltmann, C.T., Straile, D., Thackeray, S.J., Thiery, W., Urrutia-Cordero, P., Venail, P., Verburg, P., Woolway,
663 R.I., Zohary, T., Andersen, M.R., Bhattacharya, R., Hejzlar, J., Janatian, N., Kpodonu, A.T.N.K., Williamson,

664 T.J., and Wilson, H.L.: Storm impacts on phytoplankton community dynamics in lakes. *Glob. Change Biol.*, 26,
665 2756-2784, <https://doi.org/10.1111/gcb.15033>, 2020.

666 van Bergen, T.J.H.M., Barros, N., Mendonça, R., Aben, R.C.H., Althuisen, I.H.J., Huszar, V., Lamers, L.P.M.,
667 Lüring, M., Roland, F., Kosten, S.: Seasonal and diel variation in greenhouse gas emissions from an urban pond
668 and its major drivers. *Limnol. Oceanogr.*, 64, 2129-2139, <https://doi.org/10.1002/lno.11173>, 2019.

669 Varadharajan, Ch. and Hemond, H.F.: Time-series analysis of high-resolution ebullition fluxes from a stratified,
670 freshwater lake. *J. Geophys. Res.*, 117, G02004, <https://doi.org/10.1029/2011JG001866>, 2012.

671 Wanninkhof, R.: Relationship between wind speed and gas exchange over the ocean revisited. *Limnol. Oceanogr.*
672 *Methods*, 12, 351-362, <https://doi.org/10.4319/lom.2014.12.351>, 2014.

673 Wiesenburg, D.A. and Guinasso N.L.: Equilibrium solubilities of methane, carbon monoxide, and hydrogen in
674 water and sea water. *J. Chem. Eng. Data*, 24, 356-360, <https://doi.org/10.1021/je60083a006>, 1979.

675 Wik, M., Varner, R.K., Anthony, K.W., MacIntyre, S., and Bastviken, D.: Climate-sensitive northern lakes and
676 ponds are critical components of methane release. *Nat. Geosci.*, 9, 99-105, <https://doi.org/10.1038/ngeo2578>,
677 2016.

678 Xiao, Q., Zhang, M., Hu, Z., Gao, Y., Hu, Ch., Liu, Ch., Liu, S., Zhang, Z., Zhao, J., Xiao, W., and Lee, X.: Spatial
679 variations of methane emission in a large shallow eutrophic lake in subtropical climate. *J. Geophys. Res.*
680 *Biogeosci.*, 122, <https://doi.org/10.1002/2017JG003805>, 2017.

681 Yamamoto, S., Alcauskas, J.B., and Crozier, T.E. Solubility of methane in distilled water and seawater. *J. Chem.*
682 *Eng. Data*, 21, 78-80, <https://doi.org/10.1021/je60068a029>, 1976.

683 Yan, X., Xu, X., Ji, M., Zhang, Z., Wang, M., Wu, S., Wang, G., Zhang, Ch., and Liu, H.: Cyanobacteria blooms:
684 A neglected facilitator of CH₄ production in eutrophic lakes. *Sci. Total Environ.*, 651, 466-474,
685 <https://doi.org/10.1016/j.scitotenv.2018.09.197>, 2019.

686 Yang, P., Zhang, Y., Yang, H., Zhang, Y., Xu, J., Tan, L., Tong, C., and Lai, D.Y.: Large fine-scale spatiotemporal
687 variations of CH₄ diffusive fluxes from shrimp aquaculture ponds affected by organic matter supply and aeration
688 in Southeast China. *J. Geophys. Res. Biogeosci.*, 124, 1290-1307, <https://doi.org/10.1029/2019JG005025>, 2019.

689 Yang, P., Zhang, Y., Yang, H., Guo, Q., Lai, D.Y.F., Zhao, G., Li, L., and Tong, C.: Ebullition was a major
690 pathway of methane emissions from the aquaculture ponds in Southeast China. *Water Res.*, 184, 116176,
691 <https://doi.org/10.1016/j.watres.2020.116176>, 2020.

692 Yuan, J., Xiang, J., Liu, D.Y., Kang, H., He, T.H., Kim, S., Lin, Y.X., Freeman, C., and Ding, W.X.: Rapid growth
693 in greenhouse gas emissions from the adoption of industrial-scale aquaculture. *Nat. Clim. Chang.*, 9, 318-322,
694 <https://doi.org/10.1038/s41558-019-0425-9>, 2019.

695 Yuan, J., Liu, D., Xiang, J., He, T., Kang, H., and Ding, W.: Methane and nitrous oxide have separated production
696 zones and distinct emission pathways in freshwater aquaculture ponds. *Water Research*, 190, 116739,
697 <https://doi.org/10.1016/j.watres.2020.116739>, 2021.

698 Zar, J.H.: *Biostatistical analysis*. Prentice Hall, Inc., Englewood Cliffs, New York, 663 p., 1984.

699 Zhang, L., Liao, Q., Gao, R., Luo, R., Liu, Ch., Zhong, J., and Wang, Z.: Spatial variations in diffusive methane
700 fluxes and the role of eutrophication in a subtropical shallow lake. *Sci. Total Environ.*, 759, 143495,
701 <https://doi.org/10.1016/j.scitotenv.2020.143495>, 2021.

702 Zhao, J., Zhang, M., Xiao, W., Jia, L., Zhang, X., Wang, J., Zhang, Z., Xie, Y., Yini Pu, Liu, S., Feng, Z., Lee X.:
703 Large methane emission from freshwater aquaculture ponds revealed by long-term eddy covariance observation.
704 *Agric. For. Meteorol.*, 308-309, 108600, <https://doi.org/10.1016/j.agrformet.2021.108600>, 2021.
705 Zhou, Y.Q., Zhou, L., Zhang, Y.L., de Souza, J.G., Podgorski, D.C., Spencer, R.G.M., Jeppesen, E., and Davidson,
706 T.A.: Autochthonous dissolved organic matter potentially fuels methane ebullition from experimental lakes. *Water*
707 *Res.*, 166, 115048, <https://doi.org/10.1016/j.watres.2019.115048>, 2019.
708 Zuur, A.F., Ieno, E.N., Walker, N.J., Saveliev, A.A., and Smith, G.M.: *Mixed effects models and extensions in*
709 *ecology with R*. Springer, New York, USA, 574 p, <https://doi.org/10.1007/978-0-387-87458-6>, 2009.